Chemical Science

ROYAL SOCIETY OF CHEMISTRY

EDGE ARTICLE

View Article Online
View Journal | View Issue

Cite this: *Chem. Sci.*, 2020, **11**, 8184

All publication charges for this article have been paid for by the Royal Society of Chemistry

The role of neutral donor ligands in the isoselective ring-opening polymerization of *rac*-β-butyrolactone†

Xiang Dong and Jerome R. Robinson *

Isoenriched poly-3-hydroxybutyrate (P3HB) is a biodegradable material with properties similar to isotactic polypropylene, yet efficient routes to this material are lacking after 50+ years of extensive efforts in catalyst design. In this contribution, a novel lanthanum aminobisphenolate catalyst (**1-La**) can access isoenriched P3HB through the stereospecific ring-opening polymerization (ROP) of *rac*-β-butyrolactone (*rac*-BBL). Replacing the tethered donor group of a privileged supporting ligand with a non-coordinating benzyl substituent generates a catalyst whose reactivity and selectivity can be tuned with inexpensive achiral neutral donor ligands (*e.g.* phosphine oxides, OPR_3). The **1-La**/OPR_3 (R = *n*-octyl, Ph) systems display high activity and are the most isoselective homogeneous catalysts for the ROP of *rac*-BBL to date (0 °C: P_m = 0.8, TOF ~190 h^{-1}). Combined reactivity and spectroscopic studies provide insight into the active catalyst structure and ROP mechanism. Both **1-La(TPPO)$_2$** and a structurally related catalyst with a tethered donor group (**2-Y**) operate under chain-end stereocontrol; however, **2-RE** favors formation of P3HB with opposite tacticity (syndioenriched) and its ROP activity and selectivity are totally unaffected by added neutral donor ligands. Our studies uncover new roles for neutral donor ligands in stereospecific ROP, including suppression of chain-scission events, and point to new opportunities for catalyst design.

Received 25th June 2020
Accepted 15th July 2020

DOI: 10.1039/d0sc03507f

rsc.li/chemical-science

Introduction

Polyolefins enable numerous applications and benefits to society; however, there is growing concern over the immense amount of polymer waste entering landfills and waterways and their unfavorable environmental persistence.[1] Poly-3-hydroxybutyrate (P3HB, Fig. 1), the most common member of naturally occurring polyhydroxyalkanoates, is a biodegradable aliphatic polyester which can have properties similar to isotactic polypropylene and applications ranging from packaging to bio-medical applications.[2] Central to these applications is the polymer's relative stereochemistry (tacticity), which plays a critical role in its observed thermal,[3] mechanical,[3d–g,4] and degradation[3d,5] properties. For example, atactic P3HB is an amorphous material with a glass transition temperature (T_g) of ~5 °C with limited applications, while highly-enriched isotactic and syndiotactic P3HB are crystalline with melting temperatures (T_m) up to 183 °C. (*R*)-P3HB is synthesized naturally by many organisms through microbial fermentation; however, industrial production costs with this method remain high and only perfectly isotactic P3HB can be accessed.[2a,6] The high degree of crystallinity and T_m of highly-enriched isotactic or syndiotactic P3HB leads to brittle materials with processing challenges due to the proximity of the material's T_m and decomposition temperature. Alternatively, isoenriched P3HB with P_m (percentage of *meso* diads) ranging from 0.65–0.8 can suitably balance mechanical and thermal properties, making the development of efficient and economically viable methods to access this material highly desirable.[3c–f]

The stereospecific ring-opening polymerization (ROP) of *rac*-β-butyrolactone (*rac*-BBL) represents one such approach. This racemic monomer can be readily derived from abundant and

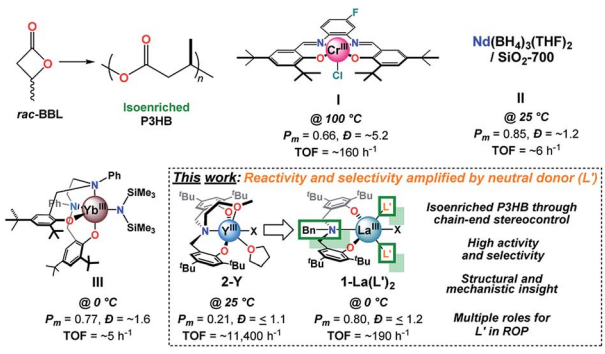

Fig. 1 Key advances in catalyst development for the ROP of *rac*-BBL to access iso-enriched P3HB with I, II, III, and the current work.

Department of Chemistry, Brown University, 324 Brook St., Providence, RI 02912, USA. E-mail: jerome_robinson@brown.edu

† Electronic supplementary information (ESI) available. CCDC 1980000–1980002. For ESI and crystallographic data in CIF or other electronic format see DOI: 10.1039/d0sc03507f

inexpensive feedstocks (*e.g.* propylene oxide and carbon monoxide),[7] displays favorable thermodynamics towards ROP thanks to its significant ring-strain ($\Delta G_p = -59.2$ kJ mol^{-1}),[8] and highly efficient catalysts have been developed for the stereospecific ROP of a variety of other lactone monomers.[2a,9] Despite these desirable attributes and a diverse array of catalysts being explored over 50+ years,[10] the development of efficient catalysts with high levels of stereocontrol has proven challenging.[9,10n,11] Many catalysts which are stereoselective for other lactone monomers (*e.g. rac*-lactide) display much lower (or no) reactivity and/or stereoselectivity towards *rac*-BBL,[10f,j,s,12] and both monomer and polymer are prone to side-reactions (*e.g.* transesterification, chain scission, deprotonation, elimination).

Extensive efforts in catalyst design have led to systems which can access syndioenriched P3HB;[3l,10n,o,13] however, few systems have led to isoenriched P3HB.[3i–k,9a,10q,11,14] Early work by Tani, Agostini, Lenz, and others identified that partial hydrolysis of alkyl aluminum species leads to catalysts which can produce a minor fraction of crystalline P3HB with properties similar to natural P3HB, albeit over prolonged reaction times (≥7 d) and with broad molecular weight distributions (*Đ*, M_w/M_n).[3i,10c,14h–k] Rieger and coworkers discovered that Cr salophen catalysts (Fig. 1, **I**) are capable of producing isoenriched P3HB with high M_n and broad *Đ* through a complex dual-site mechanism.[3j,14e,f] Thomas and coworkers developed the most isoselective heterogeneous catalyst to date ($P_m = 0.85$) by grafting $Nd(BH_4)_3(THF)_2$ to nonporous SiO_2 dehydroxylated at 700 °C (Fig. 1, **II**), but the system displays modest reactivity.[10q] Most recently, Yao and coworkers reported a series of RE^{III} salan catalysts whose stereospecific ROP is highly sensitive to N-substitution.[14g] The Yb N-Ph derivative (Fig. 1, **III**) displays modest reactivity and limited control over M_n, but is the most isoselective homogeneous catalyst to date ($P_m = 0.77$ at 0 °C). Notably, Chen and coworkers reported the ROP of a designer 8-membered diolide as an elegant alternative to circumvent selectivity challenges associated with *rac*-BBL; however, optimized catalysts produce perfectly isotactic P3HB.[3k]

Of all the catalyst platforms, trivalent rare-earth (RE^{III}) supported by tetradentate tripodal amino-bisphenolate ligands developed by Carpentier and coworkers (Fig. 1, **2-Y**) stand out as "privileged" structures due to their exceptional activity and syndioselectivity.[3l,10n,o] Though numerous covalent modifications to the ligand scaffold have been explored (*e.g.* aryloxide substitution, donor identity, tether/linker, initiator, and RE^{III}), none have provided access to isoenriched P3HB – even though such modifications have led to syndio- and iso-enriched polymers of other β-lactones.[15] Amongst these modifications, the role of the tethered donor ligand remains obscure,[16] and more broadly speaking, our understanding of how neutral achiral donor ligands influence the reactivity and stereoselectivity of ROP catalysts remains underdeveloped. In the field of asymmetric catalysis, introduction of achiral and meso neutral donor ligands can augment stereocontrol for a variety of metal-based catalysts,[17] including rare-earths,[18] in a facile and cost-effective manner. While donor-related effects in ROP have been noted,[13a,19] connections between catalyst structure and function have been limited.

Herein, we report the synthesis, characterization, and catalytic activity of RE^{III} benzyl-substituted amino-bisphenolate complexes for the isoselective ROP of *rac*-BBL. Replacing the tethered donor fragment of a tetradentate aminobisphenolate ligand with a non-coordinating benzyl substituent leads to a La catalyst whose reactivity and selectivity are amplified by the addition of inexpensive neutral achiral donor ligands (*e.g.* phosphine oxides, OPR_3). The La^{III}/OPR_3/^{i}PrOH (R: Ph, *n*-octyl) species display high activity and are the most isoselective homogeneous catalysts for the ROP of *rac*-BBL to date ($P_m = 0.8$ at 0 °C, TOF = ∼190 h^{-1}). Despite the prevalence of such ligands in the coordination chemistry of RE's[20] and other metal-ions,[21] this is the first report of added phosphine oxides enhancing catalyst reactivity or selectivity in ROP. Evidence that strong neutral donors can suppress unwanted side-reactions such as chain-scission through base-promoted elimination are also presented for the first time. Statistical analysis of P3HB microstructure confirms that **1-La(TPPO)$_2$** is the first catalyst to access isoenriched P3HB through chain-end stereocontrol. While a structurally related catalyst with a tethered donor (**2-Y**) also operates under chain-end stereocontrol, **2-RE** favor the *opposite* polymer tacticity (syndioenriched P3HB) and their performance in ROP are unaffected by added neutral donor ligands. Our studies uncover the effects of neutral donors on catalyst structure and function, and provide new opportunities for the design of catalysts for stereospecific ROP.

Results and discussion

Catalyst synthesis

The white crystalline benzyl-amino-bisphenol ligand (**H$_2$^{1}L**) was synthesized in one step by a Mannich condensation of benzyl amine, 2,4-ditertbutylphenol and paraformaldehyde in 47% yield (Scheme 1). **H$_2$^{1}L** was then treated with one equivalent of RE^{III} amide (RE^{III}: La, Y), $RE^{III}[N(SiHMe_2)_2]_3(THF)_2$, to afford the corresponding RE^{III} complexes, La^{III}(^{1}**L**)[$N(SiHMe_2)_2$]($THF)_2$ (**1-La**) and $\{Y^{III}(^1\mathbf{L})[N(SiHMe_2)_2]\}_2$ (**1-Y$_2$**), in nearly quantitative yields (Scheme 1). **1-La** is a monomer in both the solid- and solution-state as determined by single-crystal X-ray diffraction (Fig. 2) and Diffusion Ordered NMR Spectroscopy (DOSY, Fig. S10†). While X-ray quality crystals could not be grown of the

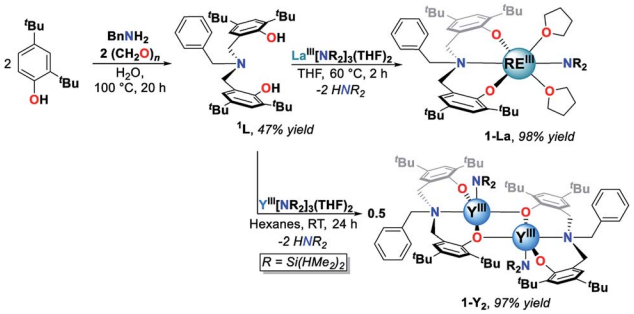

Scheme 1 Synthesis of ^{1}L and RE^{III} complexes (**1-La** and **1-Y$_2$**).

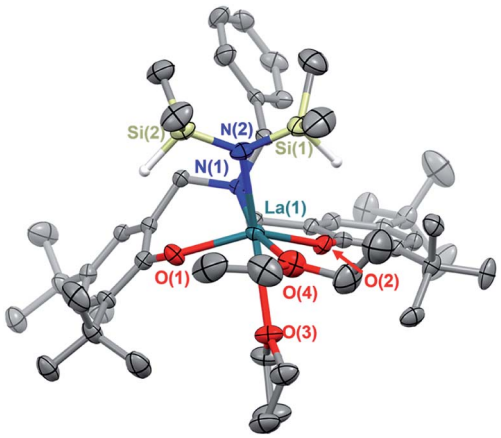

Fig. 2 Thermal ellipsoid plot of **1-La** (THF, Et_2O adduct) displayed at 50% probability.

THF adduct, slow evaporation of Et_2O solutions enabled the structural determination of the mixed THF/Et_2O adduct (Fig. 2). The geometry of the six-coordinate La^{III} center in the solid-state is best described as a distorted trigonal prism comprised of tridentate ^{1}**L**, $-N(SiHMe_2)_2$, and two coordinated solvent molecules (THF and Et_2O). ^{1}**L** adopts a propeller-like conformation at nitrogen and enforces *fac*-coordination. Agostic β-H–Si interactions (La←H–Si) were observed in the solid-state as supported by the smaller angle ∠La(1)–N(2)–Si(1) compared to ∠La(1)–N(2)–Si(2) (~15°), close La(1)–Si(1)–H contact (3.3497(13) Å), and lower energy Si–H stretch in the IR spectrum (non-agostic: 2075 cm^{-1}, agostic: 2011 cm^{-1}, Fig. S3d†).[22] Unlike **1-La**, the yttrium derivative (**1-Y$_2$**) exists as a dimer in solution as determined by ^{1}H-DOSY NMR (Fig. S11†).

Reaction optimization and neutral donor ligand effects

1-La and **1-Y$_2$** were evaluated as catalysts for the ROP of *rac*-BBL (Tables 1 and S1†). Amide initiators displayed low efficiency for the ROP of *rac*-BBL, where **1-Y$_2$** was completely inactive and **1-La** formed 35% P3HB in 48 h at RT (Table S1,† entries 1 and 5). While **1-La** was sluggish compared to Carpentier's **2-Y**,[3l,10o] formation of P3HB was encouraging as the related Sm^{III} borohydride complex supported by the propyl-amino-bisphenolate ligand reported by Mountford and coworkers was inactive for ROP of an arguably easier substrate, *rac*-lactide.[16a] Similar to other RE^{III} catalysts,[3l,10o,23] *in situ* generation of alkoxide initiators by adding one equiv. ^{i}PrOH with respect to RE^{III} (Table 1, entries 1 and 2 *vs.* Table S1,† entries 1 and 5) increased reactivity and furnished polymers with narrow M_w/M_n ($Đ$). Microstructural analysis of P3HB determined by integration of polymer C=O resonances by inverse-gated ^{13}C-NMR revealed a slight isotactic preference ($P_m = 0.57$) using **1-La**. While modest, the polymer tacticity was *opposite* that generated by **2-Y** and other amino-bisphenolate catalysts with tethered donors.[10n,o,24] Given the increased degree of coordinative unsaturation of **1-RE** compared to **2-RE** and the attributed importance of steric congestion to selectivity for other stereospecific ROP,[3l,14g,25] we posited that added neutral donor ligands could improve catalyst reactivity and selectivity through enhanced steric pressure.

We initially tested this hypothesis by screening **1-La** with two equiv. of neutral monodentate ligands. Representative classes included ethers (tetrahydrofuran, THF), tertiary amines (1,4-diazabicyclo-[2.2.2]octane, DABCO), pyridines (4-dimethylaminopyridine, DMAP), phosphines, (PPh_3), and phosphine oxides ($OPPh_3$, TPPO). Unlike some literature reports for group 13, 14, and RE^{III}-based systems,[13a,19a–i] weaker neutral ligands had a minor impact on ROP reactivity and stereoselectivity (Table 1, entries 2–5). In contrast, the harder phosphine oxide ligand, TPPO (entry 6), led to nearly quantitative conversion in 1 h (97%) and improved isoselectivity ($P_m = 0.71$). Notably [**1-La**] : [TPPO] ratios of at least 1 : 2 were needed to achieve maximum reactivity and selectivity, where a 1 : 1 ratio only led to 71% conversion and a P_m of 0.67 after 6 h (Table S1,† entries 6–9). While simple monodentate phosphine oxides have been reported as additives in asymmetric catalysis with hard metal-ions,[18a–d,26] this is the first time they have been used to enhance reactivity and/or selectivity in ROP.

Given the unprecedented and dramatic enhancement in catalyst performance, we evaluated representative classes of phosphine oxides (aromatic, aliphatic, phosphoramide, and phosphate; Table 1, entries 6–9). Electron-rich donors, such as hexamethylphosphoramide (HMPA, entry 7) and tri-octylphosphine oxide (TOPO, entry 8) increased reactivity and isoselectivity ($P_m = 0.73$ and 0.75 respectively). In contrast, triphenylphosphate ($OP(OPh)_3$, entry 9), a weaker donor, didn't increase reactivity and showed small improvements in selectivity ($P_m = 0.63$). Our results suggest both electronic and steric contributions to catalyst reactivity and selectivity, and a more comprehensive evaluation is warranted in future studies. This is affirmed by reports of stereospecific ROP of (*rac*)-lactide by RE^{III} and group 13 complexes supported by chelating alkoxides,[27] amides,[28] and pyrazolyl scorpionates[29] with *tethered* phosphine-oxides, which display varied catalyst response depending on ligand substituents. Given the diverse array of phosphine oxides that can be derived from commercially available phosphines, this represents an exciting untapped opportunity to optimize catalyst performance in stereoselective ROP.

Key polymer attributes could be tuned by adjusting reaction temperature, catalyst loading, and chain-transfer agent. Lowering the reaction temperature from RT to 0 and −30 °C with TPPO and TOPO (entries 10–15) increased catalyst isoselectivity to a maximum ($P_m = 0.80$). This represents the highest values achieved for the ROP of *rac*-BBL by a homogeneous catalyst to date.[14g] Furthermore, increased [*rac*-BBL]/[RE] ratios (400) lead to higher molecular weight P3HB with reasonable rates, identical selectivities, and narrow $Đ$ (Table 1, entries 11 and 14). Overall, **1-La**/OPR_3/^{i}PrOH systems display excellent reactivity (TOF up to 200 h^{-1}) and selectivity (P_m up to 0.80) with respect to the state-of-the-art for isoselective ROP of *rac*-BBL (P_m up to 0.77 (ref. 14g) and 0.85,[10q] TOF ~5–6 h^{-1}; Fig. 1).

Alcohols can serve as chain-transfer agents in living polymerizations to access "immortal" polymerization conditions,[30] offering further opportunities to control polymer molecular

Table 1 Influence of neutral donor ligand in the ROP of (*rac*)-BBL catalyzed by **1-RE**[a]

Entry	Cat.	[BBL]/[RE]	Ligand	Temp (°C)	Time[b] (h)	Conv.[c] (%)	$M_{n,calc}$[d] (kg mol^{-1})	$M_{n,exp}$[e] (kg mol^{-1})	$Đ$[e,f]	P_m[g]
1	**1-Y$_2$**	200	—	25	1	5	0.9	n.d.	n.d.	n.d.
2	**1-La**	200	—	25	1	21	3.6	2.9	1.04	0.57
3	**1-La**	200	DMAP	25	1	22	3.8	3.6	1.07	0.59
4	**1-La**	200	DABCO	25	1	7	1.2	n.d.	n.d.	n.d.
5	**1-La**	200	PPh_3	25	1	25	4.3	1.7	1.38	n.d.[h]
6	**1-La**	200	TPPO	25	1	97	16.7	9.6	1.18	0.71
7	**1-La**	200	HMPA	25	1	99	17.0	9.4	1.29	0.73
8	**1-La**	200	TOPO	25	1	99	17.0	9.5	1.23	0.75
9	**1-La**	200	$OP(OPh)_3$	25	1	25	4.3	1.6	1.35	0.63
10	**1-La**	200	TPPO	0	1	96	16.5	11.2	1.15	0.76
11	**1-La**	400	TPPO	0	4	77	26.5	15.3	1.20	0.75
12	**1-La**	200	TPPO	−30	24	99	17.0	11.5	1.12	0.80
13	**1-La**	200	TOPO	0	1	99	17.0	12.9	1.20	0.80
14	**1-La**	400	TOPO	0	4	96	33.1	19.2	1.09	0.80
15	**1-La**	200	TOPO	−30	6	99	17.0	13.0	1.09	0.80

[a] [BBL] = 2.4 M. [b] Reaction times not optimized. [c] Determined by ^{1}H-NMR integration of BBL and PHB methine resonances in the crude reaction mixture. [d] [BBL]/[RE]/[^{i}PrOH] × Conv. × 0.08609 + 0.0601 kg mol^{-1}. [e] Determined by gel permeation chromatography (GPC) at 30 °C in THF using polystyrene standards and corrected by Mark–Houwink factor of 0.54.[51] [f] M_w/M_n. [g] Probability of *meso*-linkages between repeat units. Determined by integration of P3HB C=O resonances using inverse gated (IG) ^{13}C-NMR. [h] 0.52 at 6 h (36% conversion).

weight.[10g,23,31] A La catalyst was isolated from a toluene solution of **1-La** and TPPO in a 1 : 2 molar ratio (*vide infra*), which displays similar reactivity in the ROP of *rac*-BBL as the *in situ* generated catalyst from adding 2 equivalents of TPPO to **1-La** (Table S2,† entry 2 and Table 1, entry 6). The ROP of *rac*-BBL (200 equiv.) catalyzed by **1-La(TPPO)$_2$** (1 equiv.) with ^{i}PrOH (1 equiv.) displayed characteristics of a living polymerization, such as narrow $Đ$ throughout the reaction and reasonable agreement between experimental and calculated M_n (Table S4 and Fig. S24†). Adding ^{i}PrOH (0–4 equiv.) to **1-La(TPPO)$_2$** maintained high catalyst activity and P_m, while producing P3HB with the expected changes in molecular weight (Table S2,† entries 1–4).

Mechanistic studies

Binding studies and catalyst characterization. We set out to isolate discrete RE^{III}–TPPO species to better understand the isoselectivity for **1-La**/OPR_3. Adding one and two equiv. of TPPO to **1-La** led to distinct mono- and bis-TPPO adducts (Fig. 3 and S7;† ^{31}P-NMR: mono: 37.5 ppm, bis: 33.3 ppm). Addition of TPPO also resulted in a downfield shift of the Si–*H* resonances, consistent with weakening and displacement of the β-H–Si interactions (La←H–Si) and TPPO coordination (Fig. 3, left).[22d] The bis-TPPO adduct displays a single significantly broadened ^{31}P signal, indicative of exchange on the NMR timescale. Isolation of crystalline bis-TPPO adducts, RE^{III}(**^{1}L**)($N(SiHMe_2)_2$)$(TPPO)_2$ (**1-RE(TPPO)$_2$**; RE^{III}: Y, La), was accomplished in high yields by adding two equiv. TPPO per RE^{III} (**1-La** or **1-Y$_2$**) in toluene followed by layering with hexanes (Fig. 4a). Although under active investigation, attempts to crystallize the mono-TPPO adduct, **1-La(TPPO)**, have only led to isolation of crystalline **1-La(TPPO)$_2$**.

The solid-state structures of **1-RE(TPPO)$_2$** were determined unambiguously by single crystal X-ray diffraction experiments (Fig. 4b, S25, and S26†). In the solid-state, **^{1}L** coordinates in a *mer*-arrangement for **1-RE(TPPO)$_2$** rather than the *fac*-arrangement for **1-La**. The isostructural compounds contain six-coordinate RE^{III} centers in a distorted octahedron with equatorial sites occupied by **^{1}L** and $–N(SiHMe_2)_2$ and axial sites occupied by TPPO. Comparison of **1-RE(TPPO)$_2$** and tethered

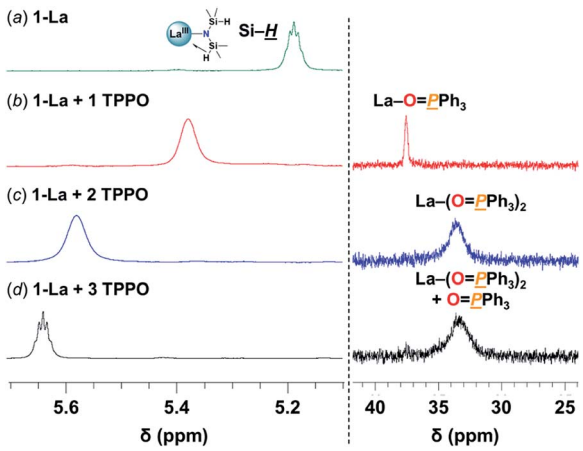

Fig. 3 Selected spectral regions of (left) ^{1}H- and (right) ^{31}P{^{1}H}-NMR studies in C_6D_6 at RT of: (a) **1-La(TPPO)$_2$** (27 mM) (b) + 1 TPPO (c) + 2 TPPO (d) + 3 TPPO. Full spectra are displayed in Fig. S7.†

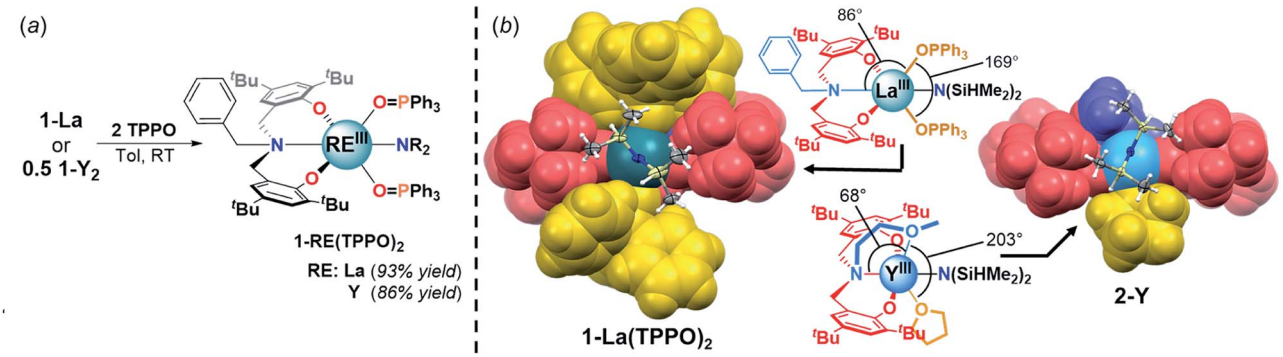

Fig. 4 (a) Synthesis of **1-RE(TPPO)$_2$**. (b) Partial space-filling diagrams comparing **1-La(TPPO)$_2$** and **2-Y**. Fragment color coding: phenolate (red), amine (blue), labile neutral donors (gold). N(SiHMe$_2$)$_2$ shown as ellipsoids (50% probability).

donor system, **2-Y**,[32] revealed largely conserved equatorial sites and significantly perturbed axial sites (Fig. 4b). In **2-Y**, the geometrically constrained tethered donor leads to a small N_L[2]–Y–O_{Me} angle (68°) and a large O_{OMe}–Y–O_{THF} angle (203°) compared to **1-La(TPPO)$_2$** (Fig. 4b, ∠N_L[1]–La–O_{TPPO}: 86°, ∠O_{TPPO}–La–O_{TPPO}: 169°). The differences in bond angles reflect increasing steric pressure from the axial donors, and suggest a plausible structural origin for the selectivity in **1-La**/OPR$_3$.

Insight into the catalyst resting state and active specie(s). With **1-La(TPPO)$_2$** in hand, we pursued further spectroscopic studies to determine relevant catalyst speciation and resting states. Variable temperature NMR experiments performed in toluene-d_8 over the range of −30 to +30 °C allowed for an estimation of TPPO exchange at the two axial sites ($\Delta G^{\ddagger}$ ~58 kJ mol^{-1}; Fig. S6†),[33] which is consistent with other RE^{III}–TPPO exchange processes reported in the literature.[34] At −30 °C, **1-La(TPPO)$_2$** displays two well-resolved ^{31}P resonances indicating slow-exchange of the two-bound TPPO at this temperature (Fig. 5a). Adding one equiv. ^{i}PrOH to **1-La(TPPO)$_2$** led to generation of HN(SiHMe$_2$)$_2$ and a La isopropoxide species as determined by ^{1}H-NMR (Fig. S16†). Bound TPPO exchanges much faster as evidenced by the nearly coalesced ^{31}P resonances at −30 °C (Fig. 5b), while a small amount of free TPPO was generated alongside another minor species (tentatively assigned as a mono-phosphine oxide species, **La(TPPO)**).

Addition of *rac*-BBL (100 equiv.) increases the signal for free TPPO significantly, while resonances associated with **La(TPPO)$_n$** (n = 1, 2) were dramatically broadened (Fig. 5c and S16†). Warming the reaction mixture from −30 °C to −15 °C and 0 °C (Fig. S17†) increased exchange of free and bound TPPO as evidenced by the increasing line-width of free TPPO (half-width at half-maximum, HWHM; 25, 80, and 150 Hz respectively), and RT experiments produced similar species (Fig. S15b†). Reactions performed at RT with one equiv. TPPO formed similar species *without* generation of free TPPO (Fig. S15a†); however, optimal catalyst reactivity and selectivity required at least two equiv. of TPPO (*vide supra*, Table S1,† entries 6–9). Taken together, our reaction optimization and *in situ* spectroscopic studies support dissociation of one equiv. TPPO from the pre-catalyst, **1-La(TPPO)$_2$**, and dynamic phosphine oxide exchange during catalysis. While **La(TPPO)** was identified as a catalyst resting state, the observed TPPO-dependent reactivity and observed speciation implicates both **La(TPPO)$_n$** (n = 1, 2) as catalytically relevant species.

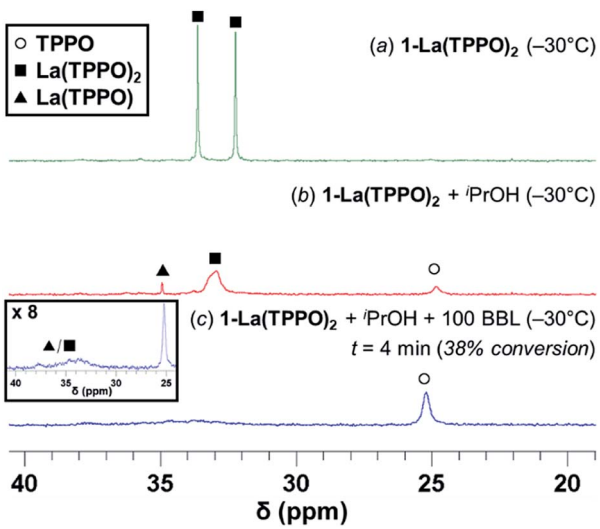

Fig. 5 ^{31}P{^{1}H}-NMR studies in toluene-d_8 at −30 °C of: (a) **1-La(TPPO)$_2$** (25 mM) (b) **1-La(TPPO)$_2$** + ^{i}PrOH (c) **1-La(TPPO)$_2$** + ^{i}PrOH + 100 equiv. (*rac*)-BBL (38% conversion). All spectra are internally referenced and intensity-normalized to PPh$_3$ (4.0 μmol; Fig. S16b†).

Stereocontrol and polymerization mechanism. Insights into the polymerization mechanism were made possible through evaluation of isolated P3HB samples (M_n, $Đ$, end-groups, statistical analysis of microstructure) and reactivity studies aimed at establishing the viability of relevant side-reactions during the ROP of *rac*-BBL using the small molecule, (*R*)-3-acetoxybutyric acid methylester [**(*R*)-3-OAcB^{Me}**].

Stereocontrol. Statistical analysis of P3HB microstructure can distinguish enantiomorphic site or chain-end stereocontrol mechanisms based on the distribution of stereoerrors.[35] Bernoullian analysis of the *meso* (*m*) and *racemic* (*r*) content in triad distributions of P3HB, $B = 4(mm)(rr)/[(rm) + (mr)]^2$, predicts a value of 1 for perfect chain-end control.[35b] A B value of 1.05 was obtained from quantitative ^{13}C-NMR of the methylene region of P3HB generated by **1-La**/TPPO at RT (Table 1, entry 6; Fig. S1†),

which is close to the theoretical prediction and confirms chain-end stereocontrol.[3l,10e,36] While chain-end stereocontrol is operative for several syndioselective catalysts,[3l,37] this is the first example with an isoselective catalyst. Other catalysts which produce isoenriched P3HB proceed through enantiomorphic site-control[3k,38] or their mechanism of stereocontrol have not yet been determined.

End-group analysis. Additional insights into the polymerization mechanism were facilitated by end-group analyses using ^{1}H-NMR and MALDI-TOF techniques. ROP of *rac*-BBL and other β-lactones catalyzed by neutral metal alkoxides commonly proceed through coordination–insertion or anionic pathways.[39] The coordination–insertion mechanism proceeds through acyl cleavage (ester and alcohol end-groups), while the anionic mechanism proceeds through alkyl cleavage (ether and carboxylate end-groups). ^{1}H-NMR spectra of isolated P3HB samples revealed the presence of an isopropyl ester end-group (Fig. S19 and S23†), while signals for an isopropyl ether were notably absent. These observations are consistent with a coordination–insertion mechanism for ROP with initiation occurring from a metal-isopropoxide.

Following a coordination–insertion mechanism, the other end-group should be a terminal secondary alcohol, which would be obtained upon hydrolysis of the propagating metal-alkoxide. As expected, the secondary alcohol end-group (–$CHOHCH_3$) was observed in a ∼1 : 1 molar ratio with respect to the ester end-group (COO^iPr). However, additional C–H resonances which correspond to a crotyl end-group were observed by ^{1}H-NMR spectroscopy (crotyl : $CHOHCH_3$: COO^iPr; ∼1 : 1 : 1). Further evidence of the crotyl end-group was established by MALDI-TOF measurements of P3HB obtained from ROP of 40 equiv. *rac*-BBL using the **1-La(TPPO)$_2$**/iPrOH catalyst system. MALDI-TOF spectra corroborated ^{1}H-NMR end-group assignments, and clearly supported crotyl end-group formation during the reaction (Fig. S22 and S23†).

Elimination studies. Generation of crotyl end-groups after polymerization could proceed through several possible pathways: (i) elimination of water, hydroxide, or oxide from the alcohol end-group under acidic or basic conditions respectively,[10g,40] (ii) thermal scission,[41] or (iii) base-induced elimination of internal ester units,[10f,42] (iv) terminal elimination from a metal alkoxide. While pathway (i) has been proposed to explain generation of crotyl end-groups after quenching polymerizations with weak acids,[3k,10g] this stands in contrast to the stability of such 3-hydroxybutanoate monomer and oligomers under strong-acid conditions.[43] Furthermore, elimination from a metal alkoxide during the reaction would convert the secondary alcohol end-group to an inactive crotyl end-group and broaden *Đ*. The relative amounts of crotyl, secondary alcohol, and isopropyl ester end groups observed (∼1 : 1 : 1, *vide supra*) and narrow *Đ* are inconsistent with expectations for this pathway. Pathway (ii) can be excluded due to the reaction temperatures evaluated in our studies (ambient or below).

Side-reactions such as deprotonation, transesterification, and elimination were proposed in early reports for the ROP of *rac*-BBL;[40b,44] however, detailed examination of the elimination pathway (iii) under mild temperatures (<100 °C) has been limited to the independent studies of Kricheldorf (K catalysts) and Coates (Zn beta-diketiminate catalysts).[10f,42a] Reactivity of internal P3HB linkages were established by the use of small molecule models, which enabled detailed identification of the resulting organic products. Despite the superior performance of many RE-based catalysts and the observation of crotyl formation in several reports,[3k,14g,24,45] investigations into elimination pathways for RE-based catalysts are notably absent. Therefore, we examined the reactivity of **1-La** and **1-La(TPPO)$_2$** with a new small molecule model, (*R*)-3-acetoxybutyric acid methylester [**(*R*)-3-OAcB^{Me}**], to establish the viability of such side-reactions [*e.g.* pathway (iii)] during ROP.

Addition of one equiv. iPrOH at RT to **1-La** and **1-La(TPPO)$_2$** cleanly generated the La isopropoxide species, **1′-La** and **1′-La(TPPO)$_2$**, and one equiv. $HN(SiHMe_2)_2$ (▲). 15 equiv. of **(*R*)-3-OAcB^{Me}** was added, and reactivity was monitored by ^{1}H-NMR after 0.5 and 7 h (Fig. 6 and S25†). Our initial expectations were that **(*R*)-3-OAcB^{Me}** would react with **1′-La** and **1′-La(TPPO)$_2$** through base-promoted elimination to form crotonate (***trans*-Crot^{Me}**), ^{i}PrOH, and a La acetate species. **1′-La** readily produced crotonate (0.5 h: 0.6 equiv.; 7 h: 1.2 equiv.); however, free ^{i}PrOH was not observed. Instead, the transesterification products, isopropyl butyrate/crotonate [**(*R*)-3-OAcB^{iPr}**/***trans*-Crot^{iPr}**] and methyl acetate (**MeOAc**), were readily identified (Fig. S25† for detailed assignments). Transesterification between the La isopropoxide and **(*R*)-3-OAcB^{Me}**/***trans*-Crot^{Me}** would lead to a La methoxide and **(*R*)-3-OAcB^{iPr}**/***trans*-Crot^{iPr}**, while transesterification between the La methoxide and the 3-acetoxy group of **(*R*)-3-OAcB^{iPr}** would generate **MeOAc** and a La 3-alkoxybutyrate species. The observed reactivity is consistent with reports of neutral La alkoxides as extremely efficient transesterification catalysts under mild conditions.[46] In addition to the aforementioned products, quantifiable amounts of free ligand (**H$_2$^{1}L**; 0.5 h: 0.1 equiv., 7 h: 0.6 equiv.) were also detected. The formation of crotonate and the direct (conjugate acids) or indirect (transesterification) products of base-promoted elimination provide clear evidence for pathway (iii) occurring readily at RT with **1′-La**.

In contrast to **1′-La**, **1′-La(TPPO)$_2$** generated less crotonate (0.5 h: 0.14 equiv., 7 h: 0.73 equiv.) and only trace amounts of **H$_2$^{1}L** after 7 h. These results highlight two additional and beneficial roles that strong neutral donor ligands (*e.g.* TPPO) can play in the ROP of *rac*-BBL. First, strong neutral donors can suppress elimination, as evidenced by the significantly decreased amount of crotonate formed with **1′-La(TPPO)$_2$** compared to **1′-La**. Supressing this side-reaction is critical, as the resulting La carboxylates would be inactive towards coordination–insertion ROP at RT (*i.e.* dormant chains), while chain-scission would also broaden *Đ* and lower M_n. Second, strong neutral donors can effectively suppress the kinetic basicity of the supporting ligand, as evidenced by significant amounts of **H$_2$^{1}L** generated with **1′-La**. While RE aryloxides have been leveraged as efficient multi-functional catalysts through cooperative Lewis-acid/Lewis-base reactions (*e.g.* Michael, aldol, hydrophosphination),[47] RE aryloxides have been considered as innocent supporting ligands for the ROP of *rac*-BBL. Although rapid transesterification was observed for **1-La** and **1-La(TPPO)$_2$**,

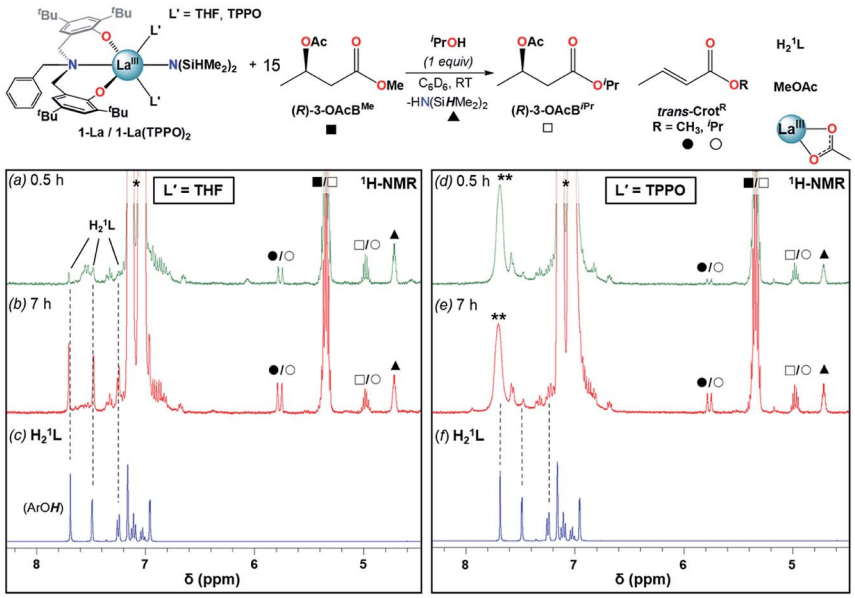

Fig. 6 Reactivity studies of **1-La** and **1-La(TPPO)$_2$** in the presence of one equiv. ^{i}PrOH and 15 equiv. **(*R*)-3-OAcB^{Me}** followed by ^{1}H-NMR after 0.5 h (a and d), 7 h (b and e). Dashed lines provided to help track the formation of $H_2{}^1$**L** (c and f) during the reaction time course. * = toluene (from ^{i}PrOH stock solution), ** = TPPO. Detailed assignments of full spectra provided as Fig. S25.†

the low $Đ$ and high P_m support that this side-reaction is less significant under catalytic conditions. The pronounced tendency towards transesterification should correspond to the lower steric-bulk of the methyl ester found in **(*R*)-3-OAcB^{Me}** compared to the more hindered ester linkages in P3HB.

*The effect of neutral donors on ROP catalyzed by **1-RE** and **2-RE**.* Given the observed benefits of adding strong neutral donor ligands to **1-RE** (*vide supra*), we set out to evaluate whether similar enhancements would occur in structurally related catalysts with a tethered donor group (**2-Y** and **2-La**). This was motivated by reports of solvent-dependent[10o] and tethered-donor dependent[24,48] ROP reactivity for **2-RE** and its derivatives. ^{1}H- and ^{31}P{^{1}H}-NMR studies indicate that TPPO readily binds to **2-RE** in solution (Fig. S18†); however, unlike **1-RE**, rates and selectivity for the ROP of *rac*-BBL were totally unaffected by added TPPO (Table 2, entries 3–5 and 8–10). While initially unanticipated, we suspect this is due to the much high concentrations of the weaker donor ligands (solvent) compared to our studies (two equiv.).[3l,10o] Under our experimental conditions, the tethered donor of **2-RE** dominates the observed reactivity and stereoselectivity, indicating that propagation from the corresponding TPPO adducts of **2-RE** is a higher energy pathway.

The presence or absence of a tethered donor also manifests opposite size-dependent reactivity and selectivity trends for **1-RE** and **2-RE**. Smaller ions are more reactive and selective for **2-RE**,[3l,25,37b] while larger ions are more reactive for **1-RE**/OPR$_3$. While both catalysts display chain-end stereocontrol and feature labile coordination sites *cis* to an initiator (two for **1-RE**, one for **2-RE**), amplified selectivity is only observed with the largest and most coordinatively unsaturated catalyst, **1-La**. Furthermore, the presence (**2-RE**) or absence (**1-RE**/OPR$_3$) of a tethered donor group favors opposite polymer tacticities (**2-RE**: syndio, **1-RE**: iso).

Proposed mechanism. Given the results of our catalytic and mechanistic studies, we propose the following mechanism for the ROP of *rac*-BBL catalyzed by **1-La** & **1-La(TPPO)$_2$** (Fig. 7; L′ = THF or TPPO). Addition of ^{i}PrOH to **1-La** or **1-La(TPPO)$_2$** leads to a highly reactive initiator, **1′-La** or **1′-La(TPPO)$_2$**. Ligand exchange of L′ for *rac*-BBL generates **A**, which can then undergo insertion of the La alkoxide to generate **B**. Ring-opening would lead to **C**, which is involved in two competing ligand-exchange equilibria that gates productive (propagation) and unproductive (elimination) pathways. Upon binding of one equiv. L′ to **C**, the catalytic cycle is successfully completed with the regeneration of **1′-La**. Our low-temperature NMR studies of **1-La(TPPO)$_2$** support a mono-TPPO resting state during ROP, while our catalytic studies indicate that more than one equiv. of TPPO is required to achieve maximum rate and selectivity enhancements (Table S1,† entries 6–9). While we have depicted **A**, **B**, and **C** as mono-L′ adducts, we cannot exclude the possibility that one or more of these intermediates may be bis-L′ adducts.

Alternatively, at high reaction conversions or with weaker donor ligands, binding of ester linkages to **C** may become competitive with L′ to form the key intermediate for base-promoted elimination, **D**. Chain cleavage through elimination would generate two polymer fragments that are inactive for further ROP at RT: (i) a terminated polymer with ester and crotyl end-groups, and (ii) a dormant polyester chain terminated by rare-earth carboxylate and secondary alcohol end-groups. With weak and sterically unencumbered donors (*e.g.* L′ = THF), both the propagating alkoxide chain and ^{1}**L** could act as competent bases, while the kinetic basicity of ^{1}**L** is suppressed with strong and bulky neutral donors (*e.g.* L′ = TPPO). While intermediate **D**

Table 2 Effects of TPPO on **1-RE** and **2-RE** ROP activity with *rac*-BBL

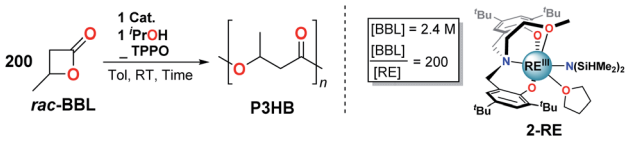

Entry	[Cat.]	[TPPO]/[RE]	Time[a] (h)	Conv.[b] (%)	$M_{n,exp}$[c] (kg mol^{-1})	$Đ$[c,d]	P_m[e]
1	**1-La**	0	24	40	2.2	1.23	0.57
2	**1-La**	2	1	97	9.6	1.18	0.71
3	**2-La**	0	24	22	1.4	1.17	0.45
4	**2-La**	1	24	21	1.6	1.14	0.49
5	**2-La**	2	24	21	1.7	1.16	0.48
6	**1-Y$_2$**	0	24	33	5.9	1.15	0.55
7	**1-Y$_2$**	2	3	95	14.0	1.18	0.51
8	**2-Y**	0	1	91	14.2	1.16	0.22
9	**2-Y**	1	1	99	17.6	1.12	0.22
10	**2-Y**	2	1	99	15.9	1.14	0.22

[a] Reaction times not optimized. [b] Determined by ^{1}H-NMR integration of BBL and PHB methine resonances in the crude reaction mixture. [c] Determined by gel permeation chromatography (GPC) at 30 °C in THF using polystyrene standards and corrected by Mark–Houwink factor of 0.54.[51] [d] M_w/M_n. [e] Probability of *meso*-linkages between repeat units. Determined by integration of P3HB C=O resonances using inverse gated (IG) ^{13}C-NMR.

is depicted with coordination of a neighboring polyester chain, we expect that both intra- and inter-molecular pathways are viable.

While the exact origin of the unique isoselectivity remains unresolved, we hypothesize that strong neutral donors such as TPPO lead to a sterically crowded axial environment in **1-La(TPPO)$_2$** compared to **1-La** and **2-RE** (Fig. 7). Non-covalent C–H···π (arene) interactions between ligand and substrate have been proposed to explain the high syndioselectivity for the ROP of *rac*-BBL with a yttrium catalyst supported by a cumyl-substituted tetradentate amino-bisphenolate ligand.[37b] In contrast, we observed similar reactivity and selectivity with phosphine oxides containing aromatic (TPPO) or aliphatic (TOPO) substituents, which suggests other origins for the unique isoselective chain-end stereocontrol. Rieger and coworkers recently carried out an extensive computational study investigating the ROP of *rac*-BBL catalyzed by **2-Y**.[25] The syndioselective pathway is favored kinetically and thermodynamically by the propagating P3HB chain adopting a κ^3 binding mode. The authors suggest that alternative P3HB binding modes (*e.g.* κ^1 or κ^2) may lead to iso-enriched P3HB. Such intermediates (Fig. 7: **A** or **B**) could be favored by the stronger binding and enhanced steric bulk of phosphine oxides, opening up new pathways that are disfavored for **2-Y**.

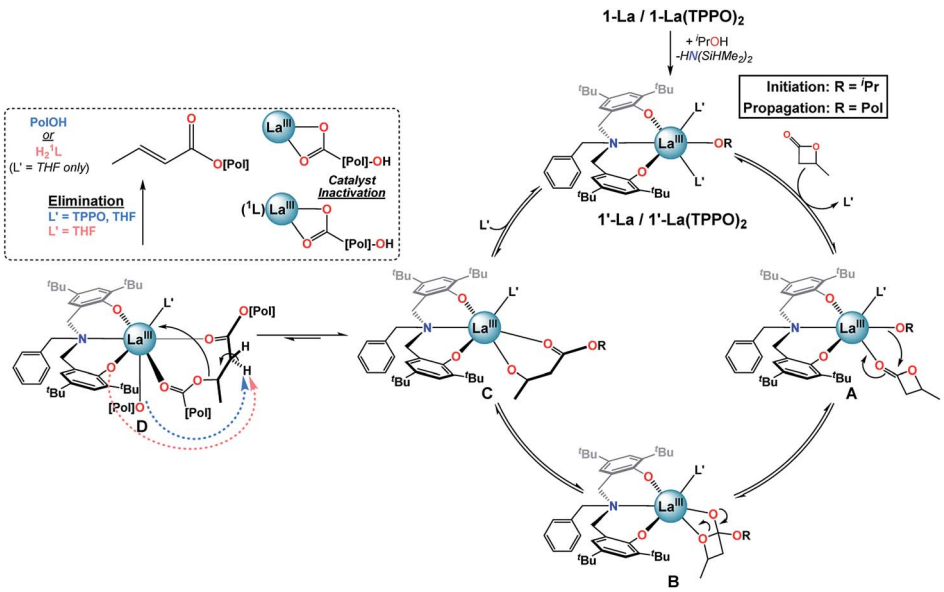

Fig. 7 Proposed mechanism for the ROP of *rac*-BBL catalyzed by **1-La** and **1-La(TPPO)$_2$**.

Finally, our mechanistic studies uncover new roles for neutral donor ligands in ROP. Previous studies have provided evidence for decreased transesterification[19a,b,e,49] and control of catalyst aggregation state[19h,j,49a,50] with added neutral donor ligands; however, their role in suppressing base-promoted elimination (*i.e.* crotyl end-group) was previously unknown. Our results suggest that neutral donor groups play a critical role in suppressing or shifting ligand-exchange equilibria for both productive and non-productive pathways in the ROP of *rac*-BBL, and addition of these simple ligands provide a facile and inexpensive way to further modulate catalyst performance.

Conclusions

In summary, we have synthesized, characterized, and evaluated the reactivity of novel benzyl-substituted amino-bisphenolate rare-earth complexes, **1-RE**, as catalysts for the isoselective ROP of *rac*-BBL. **1-RE** display ROP rates and selectivities that are tuned by the identity of exogenous neutral donor ligands (*e.g.* OPR_3). **1-La**/OPR_3/^{i}PrOH display excellent reactivity and selectivity (P_m = 0.8 at 0 °C, TOF = ~190 h^{-1}), and are the most isoselective homogeneous catalysts for ROP of *rac*-BBL (R: *n*-octyl, Ph). The use of simple monodentate OPR_3 to enhance catalyst performance in stereoselective ROP is unprecedented, and the relative ease and accessibility to a diverse array of phosphine oxides makes this an attractive and operationally simple strategy to further optimize catalyst performance.

Our preliminary mechanistic studies indicate that (i) **1-La(TPPO)$_2$** is a precatalyst for the isoselective ROP of *rac*-BBL, (ii) **La(TPPO)$_n$** (n = 1, 2) are implicated as catalytically relevant species, (iii) isoselective ROP proceeds with chain-end stereocontrol through a coordination–insertion mechanism, and (iv) addition of neutral donor ligands can suppress elimination side-reactions. This is the first investigation into elimination pathways of RE-based catalysts in the ROP of *rac*-BBL, and **1-La(TPPO)$_2$** is the first catalyst to access isoenriched P3HB with chain-end stereocontrol. While structurally related catalysts with a tethered donor group (**2-RE**) also operate under chain-end stereocontrol, ROP activity and selectivity of **2-RE** (i) are unaffected by added neutral donor ligands and (ii) display opposite stereoselectivity (syndioselective) compared to **1-La**/OPR_3. Our study uncovers new roles for neutral donor ligands in stereospecific ROP, and begins to connect their effect on catalyst structure and function. Removing the tethered donor fragment and increasing axial steric bulk with strong neutral donor ligands favors isoenriched P3HB. Similar donor-related enhancements may require catalysts with enhanced metal accessibility (*i.e.* several labile coordination sites), and highlight new opportunities in catalyst design and optimization. Extension of this approach to other catalysts for stereoselective ROP, the stereoselective synthesis of other oxygenated (co)polymers, and further mechanistic studies are currently underway.

Conflicts of interest

There are no conflicts to declare.

Acknowledgements

We thank Brown University for support of this research. We thank Savannah Snyder and Chrys Wesdemiotis, University of Akron, for performing high-resolution MALDI-TOF measurements used for chain-end analysis. We thank Patrick J. Carroll, Eric J. Schelter, and Chris R. Graves for helpful discussions. X. D. and J. R. R. are inventors on U.S. patent application 62/950,702 submitted by Brown University, which covers the catalysts and process described herein.

Notes and references

1 (*a*) R. Geyer, J. R. Jambeck and K. L. Law, *Sci. Adv.*, 2017, **3**, e1700782; (*b*) B. Worm, H. K. Lotze, I. Jubinville, C. Wilcox and J. Jambeck, *Annu. Rev. Environ. Resour.*, 2017, **42**, 1–26; (*c*) A. A. de Souza Machado, W. Kloas, C. Zarfl, S. Hempel and M. C. Rillig, *Global Change Biol.*, 2018, **24**, 1405–1416; (*d*) S. Chiba, H. Saito, R. Fletcher, T. Yogi, M. Kayo, S. Miyagi, M. Ogido and K. Fujikura, *Marine Policy*, 2018, **96**, 204–212.

2 (*a*) B. Rieger, A. Künkel, G. W. Coates, R. Reichardt, E. Dinjus and T. A. Zevaco, *Synthetic Biodegradable Polymers*, Springer Berlin, Berlin, 2014, pp. 49–90; (*b*) R. A. Gross and B. Kalra, *Science*, 2002, **297**, 803–807; (*c*) E. Bugnicourt, P. Cinelli, A. Lazzeri and V. Alvarez, *eXPRESS Polym. Lett.*, 2014, **8**, 791–808; (*d*) Y. Zhu, C. Romain and C. K. Williams, *Nature*, 2016, **540**, 354; (*e*) Z. A. Raza, S. Abid and I. M. Banat, *Int. Biodeterior. Biodegrad.*, 2018, **126**, 45–56; (*f*) A. Sangroniz, J.-B. Zhu, X. Tang, A. Etxeberria, E. Y. X. Chen and H. Sardon, *Nat. Commun.*, 2019, **10**, 3559.

3 (*a*) Z. Jedliński, M. Kowalczuk, P. Kurcok, L. Brzoskowska and J. Franek, *Macromol. Chem. Phys.*, 1987, **188**, 1575–1582; (*b*) S. Bloembergen, D. A. Holden, T. L. Bluhm, G. K. Hamer and R. H. Marchessault, *Macromolecules*, 1989, **22**, 1656–1663; (*c*) N. Tanahashi and Y. Doi, *Macromolecules*, 1991, **24**, 5732–5733; (*d*) Y. Kumagai and Y. Doi, *Macromol. Rapid Commun.*, 1992, **13**, 179–183; (*e*) H. Abe, I. Matsubara, Y. Doi, Y. Hori and A. Yamaguchi, *Macromolecules*, 1994, **27**, 6018–6025; (*f*) M. Haslböck, M. Klotz, J. Sperl, V. Sieber, C. Zollfrank and D. Van Opdenbosch, *Macromolecules*, 2019, **52**, 5407–5418; (*g*) H. R. Kricheldorf and S. Eggerstedt, *Macromolecules*, 1997, **30**, 5693–5697; (*h*) C. Jaimes, M. Arcana, A. Brethon, A. Mathieu, F. Schue and J. M. Desimone, *Eur. Polym. J.*, 1998, **34**, 175–185; (*i*) B. Wu and R. W. Lenz, *Macromolecules*, 1998, **31**, 3473–3477; (*j*) M. Zintl, F. Molnar, T. Urban, V. Bernhart, P. Preishuber-Pflügl and B. Rieger, *Angew. Chem., Int. Ed.*, 2008, **47**, 3458–3460; (*k*) X. Tang and E. Y. X. Chen, *Nat. Commun.*, 2018, **9**, 1–11; (*l*) N. Ajellal, M. Bouyahyi, A. Amgoune, C. M. Thomas, A. Bondon, I. Pillin, Y. Grohens and J.-F. Carpentier, *Macromolecules*, 2009, **42**, 987–993.

4 S. Kusaka, T. Iwata and Y. Doi, *J. Macromol. Sci., Part A: Pure Appl. Chem.*, 1998, **35**, 319–335.

5 (*a*) J. E. Kemnitzer, S. P. McCarthy and R. A. Gross, *Macromolecules*, 1992, **25**, 5927–5934; (*b*) H. Abe and

Y. Doi, *Macromolecules*, 1996, **29**, 8683–8688; (*c*) M. R. Timmins, R. W. Lenz, P. J. Hocking, R. H. Marchessault and R. C. Fuller, *Macromol. Chem. Phys.*, 1996, **197**, 1193–1215; (*d*) Y. He, X. Shuai, K.-i. Kasuya, Y. Doi and Y. Inoue, *Biomacromolecules*, 2001, **2**, 1045–1051; (*e*) S. I. Vagin, A. Kronast, P. T. Altenbuchner, F. Adams, C. Sinkel, P. Deglmann, R. Loos, T. Schuffenhauer, B. Sommer, T. Brück and B. Rieger, *Polym. Degrad. Stab.*, 2017, **143**, 176–185.

6 (*a*) Y. K. Leong, P. L. Show, C. W. Ooi, T. C. Ling and J. C.-W. Lan, *J. Biotechnol.*, 2014, **180**, 52–65; (*b*) J. Możejko-Ciesielska and R. Kiewisz, *Microbiol. Res.*, 2016, **192**, 271–282.

7 (*a*) Y. D. Y. L. Getzler, V. Mahadevan, E. B. Lobkovsky and G. W. Coates, *J. Am. Chem. Soc.*, 2002, **124**, 1174–1175; (*b*) F. Molnar, G. A. Luinstra, M. Allmendinger and B. Rieger, *Chem.–Eur. J.*, 2003, **9**, 1273–1280; (*c*) J. W. Kramer, E. B. Lobkovsky and G. W. Coates, *Org. Lett.*, 2006, **8**, 3709–3712.

8 A. Duda and S. Penczek, Mechanisms of Aliphatic Polyester Formation, in *Biopolymers Online*, Wiley VCH, 2002, vol. 3b, pp. 371–429.

9 (*a*) C. M. Thomas, *Chem. Soc. Rev.*, 2010, **39**, 165–173; (*b*) S. M. Guillaume, E. Kirillov, Y. Sarazin and J.-F. Carpentier, *Chem.–Eur. J.*, 2015, **21**, 7988–8003; (*c*) H. Li, R. M. Shakaroun, S. M. Guillaume and J.-F. Carpentier, *Chem.–Eur. J.*, 2020, **26**, 128–138.

10 Select representative examples. *Historical examples*: (*a*) H. K. Hall and A. K. Schneider, *J. Am. Chem. Soc.*, 1958, **80**, 6409–6412; (*b*) S. Inoue, Y. Tomoi, T. Tsuruta and J. Furukawa, *Macromol. Chem. Phys.*, 1961, **48**, 229–233; (*c*) D. E. Agostini, J. B. Lando and J. R. Shelton, *J. Polym. Sci., Part A-1: Polym. Chem.*, 1971, **9**, 2775–2787; (*d*) T. Yasuda, T. Aida and S. Inoue, *Macromol. Rapid Commun.*, 1982, **3**, 585–588; (*e*) J. E. Kemnitzer, S. P. McCarthy and R. A. Gross, *Macromolecules*, 1993, **26**, 6143–6150; *Zn*: (*f*) L. R. Rieth, D. R. Moore, E. B. Lobkovsky and G. W. Coates, *J. Am. Chem. Soc.*, 2002, **124**, 15239–15248; (*g*) M. Shaik, J. Peterson and G. Du, *Macromolecules*, 2019, **52**, 157–166; *group I, II, 13*: (*h*) J. Gao, D. Zhu, W. Zhang, G. A. Solan, Y. Ma and W.-H. Sun, *Inorg. Chem. Front.*, 2019, **6**, 2619–2652; (*i*) S. M. Quan and P. L. Diaconescu, *Chem. Commun.*, 2015, **51**, 9643–9646; (*j*) T. Ebrahimi, S. G. Hatzikiriakos and P. Mehrkhodavandi, *Macromolecules*, 2015, **48**, 6672–6681; group IV: (*k*) B. J. Jeffery, E. L. Whitelaw, D. Garcia-Vivo, J. A. Stewart, M. F. Mahon, M. G. Davidson and M. D. Jones, *Chem. Commun.*, 2011, **47**, 12328–12330; *Au*: (*l*) E. Brulé, S. Gaillard, M.-N. Rager, T. Roisnel, V. Guérineau, S. P. Nolan and C. M. Thomas, *Organometallics*, 2011, **30**, 2650–2653; RE^{III} (*m*) D. M. Lyubov, A. O. Tolpygin and A. A. Trifonov, *Coord. Chem. Rev.*, 2019, **392**, 83–145; (*n*) J.-F. Carpentier, *Organometallics*, 2015, **34**, 4175–4189; (*o*) A. Amgoune, C. M. Thomas, S. Ilinca, T. Roisnel and J.-F. Carpentier, *Angew. Chem., Int. Ed.*, 2006, **45**, 2782–2784; (*p*) A. Alaaeddine, A. Amgoune, C. M. Thomas, S. Dagorne, S. Bellemin-Laponnaz and J.-F. Carpentier, *Eur. J. Inorg. Chem.*, 2006, **2006**, 3652–3658; (*q*) N. Ajellal, G. Durieux, L. Delevoye, G. Tricot, C. Dujardin, C. M. Thomas and R. M. Gauvin, *Chem. Commun.*, 2010, **46**, 1032–1034; *organocatalysts*: (*r*) M. K. Kiesewetter, E. J. Shin, J. L. Hedrick and R. M. Waymouth, *Macromolecules*, 2010, **43**, 2093–2107; (*s*) W. Jeong, J. L. Hedrick and R. M. Waymouth, *J. Am. Chem. Soc.*, 2007, **129**, 8414–8415; (*t*) C. G. Jaffredo, J. F. Carpentier and S. M. Guillaume, *Macromol. Rapid Commun.*, 2012, **33**, 1938–1944.

11 J.-F. Carpentier, *Macromol. Rapid Commun.*, 2010, **31**, 1696–1705.

12 (*a*) M. Cheng, A. B. Attygalle, E. B. Lobkovsky and G. W. Coates, *J. Am. Chem. Soc.*, 1999, **121**, 11583–11584; (*b*) B. M. Chamberlain, M. Cheng, D. R. Moore, T. M. Ovitt, E. B. Lobkovsky and G. W. Coates, *J. Am. Chem. Soc.*, 2001, **123**, 3229–3238; (*c*) A. F. Douglas, B. O. Patrick and P. Mehrkhodavandi, *Angew. Chem., Int. Ed.*, 2008, **47**, 2290–2293; (*d*) T. R. Jensen, L. E. Breyfogle, M. A. Hillmyer and W. B. Tolman, *Chem. Commun.*, 2004, 2504–2505; (*e*) A. P. Dove, H. Li, R. C. Pratt, B. G. G. Lohmeijer, D. A. Culkin, R. M. Waymouth and J. L. Hedrick, *Chem. Commun.*, 2006, 2881–2883; (*f*) P. Hormnirun, E. L. Marshall, V. C. Gibson, A. J. P. White and D. J. Williams, *J. Am. Chem. Soc.*, 2004, **126**, 2688–2689; (*g*) P. Hormnirun, E. L. Marshall, V. C. Gibson, R. I. Pugh and A. J. P. White, *Proc. Natl. Acad. Sci. U. S. A.*, 2006, **103**, 15343–15348; (*h*) E. D. Cross, L. E. N. Allan, A. Decken and M. P. Shaver, *J. Polym. Sci., Part A: Polym. Chem.*, 2013, **51**, 1137–1146; (*i*) C. Bakewell, A. J. P. White, N. J. Long and C. K. Williams, *Angew. Chem., Int. Ed.*, 2014, **53**, 9226–9230; (*j*) C. Bakewell, A. J. P. White, N. J. Long and C. K. Williams, *Inorg. Chem.*, 2015, **54**, 2204–2212; (*k*) K. Nie, W. Gu, Y. Yao, Y. Zhang and Q. Shen, *Organometallics*, 2013, **32**, 2608–2617.

13 (*a*) J. S. Klitzke, T. Roisnel, E. Kirillov, O. d. L. Casagrande and J.-F. Carpentier, *Organometallics*, 2014, **33**, 309–321; (*b*) J. Fang, M. J. L. Tschan, T. Roisnel, X. Trivelli, R. M. Gauvin, C. M. Thomas and L. Maron, *Polym. Chem.*, 2013, **4**, 360–367; (*c*) H. Wang, J. Guo, Y. Yang and H. Ma, *Dalton Trans.*, 2016, **45**, 10942–10953.

14 (*a*) T. Takeichi, Y. Hieda and Y. Takayama, *Polym. J.*, 1988, **20**, 159–162; (*b*) A. Le Borgne and N. Spassky, *Polymer*, 1989, **30**, 2312–2319; (*c*) N. Spassky, C. Pluta, V. Simic, M. Thiam and M. Wisniewski, *Macromol. Symp.*, 1998, **128**, 39–51; (*d*) M. Terrier, E. Brule, M. J. Vitorino, N. Ajellal, C. Robert, R. M. Gauvin and C. M. Thomas, *Macromol. Rapid Commun.*, 2011, **32**, 215–219; (*e*) R. Reichardt, S. Vagin, R. Reithmeier, A. K. Ott and B. Rieger, *Macromolecules*, 2010, **43**, 9311–9317; (*f*) S. Vagin, M. Winnacker, A. Kronast, P. T. Altenbuchner, P. Deglmann, C. Sinkel, R. Loos and B. Rieger, *ChemCatChem*, 2015, **7**, 3963–3971; (*g*) Z. Zhuo, C. Zhang, Y. Luo, Y. Wang, Y. Yao, D. Yuan and D. Cui, *Chem. Commun.*, 2018, **54**, 11998–12001; (*h*) H. Tani, S. Yamashita and K. Teranishi, *Polym. J.*, 1972, **3**, 417–418; (*i*) M. Iida, T. Araki, K. Teranishi and H. Tani, *Macromolecules*, 1977,

10, 275–284; (*j*) K. Teranishi, M. Iida, T. Araki, S. Yamashita and H. Tani, *Macromolecules*, 1974, **7**, 421–427; (*k*) R. A. Gross, Y. Zhang, G. Konrad and R. W. Lenz, *Macromolecules*, 1988, **21**, 2657–2668.

15 R. Ligny, M. M. Hänninen, S. M. Guillaume and J.-F. Carpentier, *Angew. Chem., Int. Ed.*, 2017, **56**, 10388–10393.

16 (*a*) H. E. Dyer, S. Huijser, N. Susperregui, F. Bonnet, A. D. Schwarz, R. Duchateau, L. Maron and P. Mountford, *Organometallics*, 2010, **29**, 3602–3621; (*b*) L.-Q. Deng, Y.-X. Zhou, X. Tao, Y.-L. Wang, Q.-S. Hu, P. Jin and Y.-Z. Shen, *J. Organomet. Chem.*, 2014, **749**, 356–363.

17 P. J. Walsh, A. E. Lurain and J. Balsells, *Chem. Rev.*, 2003, **103**, 3297–3344.

18 (*a*) T. Nemoto, T. Ohshima, K. Yamaguchi and M. Shibasaki, *J. Am. Chem. Soc.*, 2001, **123**, 2725–2732; (*b*) H. Kakei, R. Tsuji, T. Ohshima and M. Shibasaki, *J. Am. Chem. Soc.*, 2005, **127**, 8962–8963; (*c*) H. Kakei, R. Tsuji, T. Ohshima, H. Morimoto, S. Matsunaga and M. Shibasaki, *Chem.–Asian J.*, 2007, **2**, 257–264; (*d*) K. Hara, S.-Y. Park, N. Yamagiwa, S. Matsunaga and M. Shibasaki, *Chem.–Asian J.*, 2008, **3**, 1500–1504; (*e*) J. R. Robinson, J. Yadav, X. Fan, G. R. Stanton, E. J. Schelter, M. A. Pericàs and P. J. Walsh, *Adv. Synth. Catal.*, 2014, **356**, 1243–1254.

19 *Reactivity*: (*a*) P. Dubois, I. Barakat, R. Jerome and P. Teyssie, *Macromolecules*, 1993, **26**, 4407–4412; (*b*) P. Dubois, R. Jérôme and P. Teyssié, *Polym. Prepr. (Am. Chem. Soc., Div. Polym. Chem.)*, 1994, **35**, 536–537; (*c*) P. Dubois, N. Ropson, R. Jérôme and P. Teyssié, *Macromolecules*, 1996, **29**, 1965–1975; (*d*) L. S. Boffa and B. M. Novak, *Macromolecules*, 1997, **30**, 3494–3506; (*e*) P. Degée, P. Dubois, S. Jacobsen, H.-G. Fritz and R. Jérôme, *J. Polym. Sci., Part A: Polym. Chem.*, 1999, **37**, 2413–2420; (*f*) P. Ravi, T. Gröb, K. Dehnicke and A. Greiner, *Macromolecules*, 2001, **34**, 8649–8653; *selectivity*: (*g*) M. H. Chisholm, J. C. Gallucci and K. Phomphrai, *Inorg. Chem.*, 2004, **43**, 6717–6725; (*h*) P. Horeglad, P. Kruk and J. Pécaut, *Organometallics*, 2010, **29**, 3729–3734; (*i*) M. H. Chisholm, K. Choojun, A. S. Chow and G. Fraenkel, *Angew. Chem., Int. Ed.*, 2013, **52**, 3264–3266; (*j*) P. Horeglad, G. Szczepaniak, M. Dranka and J. Zachara, *Chem. Commun.*, 2012, **48**, 1171–1173.

20 A. W. G. Platt, *Coord. Chem. Rev.*, 2017, **340**, 62–78.

21 M. B. Smith, Phosphorus Ligands, in *Reference Module in Chemistry, Molecular Sciences and Chemical Engineering*, Elsevier, 2013.

22 (*a*) R. Anwander, O. Runte, J. Eppinger, G. Gerstberger, E. Herdtweck and M. Spiegler, *J. Chem. Soc., Dalton Trans.*, 1998, 847–858; (*b*) H. M. Dietrich, C. Meermann, K. W. Törnroos and R. Anwander, *Organometallics*, 2006, **25**, 4316–4321; (*c*) H. F. Yuen and T. J. Marks, *Organometallics*, 2008, **27**, 155–158; (*d*) C. Meermann, G. Gerstberger, M. Spiegler, K. W. Törnroos and R. Anwander, *Eur. J. Inorg. Chem.*, 2008, **2008**, 2014–2023; (*e*) Y. Chapurina, J. Klitzke, O. d. L. Casagrande Jr, M. Awada, V. Dorcet, E. Kirillov and J.-F. Carpentier, *Dalton Trans.*, 2014, **43**, 14322–14333.

23 H. Ma and J. Okuda, *Macromolecules*, 2005, **38**, 2665–2673.

24 K. Nie, L. Fang, Y. Yao, Y. Zhang, Q. Shen and Y. Wang, *Inorg. Chem.*, 2012, **51**, 11133–11143.

25 P. T. Altenbuchner, A. Kronast, S. Kissling, S. I. Vagin, E. Herdtweck, A. Pöthig, P. Deglmann, R. Loos and B. Rieger, *Chem.–Eur. J.*, 2015, **21**, 13609–13617.

26 L. Wang, D. Yang, D. Li, X. Liu, P. Wang, K. Wang, H. Zhu, L. Bai and R. Wang, *Angew. Chem., Int. Ed.*, 2018, **57**, 9088–9092.

27 (*a*) P. L. Arnold, J.-C. Buffet, R. P. Blaudeck, S. Sujecki, A. J. Blake and C. Wilson, *Angew. Chem., Int. Ed.*, 2008, **47**, 6033–6036; (*b*) P. L. Arnold, J. C. Buffet, R. Blaudeck, S. Sujecki and C. Wilson, *Chem.–Eur. J.*, 2009, **15**, 8241–8250; (*c*) J.-C. Buffet, J. Okuda and P. L. Arnold, *Inorg. Chem.*, 2010, **49**, 419–426.

28 (*a*) R. H. Platel, A. J. P. White and C. K. Williams, *Chem. Commun.*, 2009, 4115–4117; (*b*) R. H. Platel, A. J. P. White and C. K. Williams, *Inorg. Chem.*, 2011, **50**, 7718–7728.

29 (*a*) Z. Zhang and D. Cui, *Chem.–Eur. J.*, 2011, **17**, 11520–11526; (*b*) Z. Mou, B. Liu, X. Liu, H. Xie, W. Rong, L. Li, S. Li and D. Cui, *Macromolecules*, 2014, **47**, 2233–2241.

30 S. Asano, T. Aida and S. Inoue, *J. Chem. Soc., Chem. Commun.*, 1985, 1148–1149.

31 N. Ajellal, J.-F. Carpentier, C. Guillaume, S. M. Guillaume, M. Helou, V. Poirier, Y. Sarazin and A. Trifonov, *Dalton Trans.*, 2010, **39**, 8363–8376.

32 C.-X. Cai, L. Toupet, C. W. Lehmann and J.-F. Carpentier, *J. Organomet. Chem.*, 2003, **683**, 131–136.

33 H. Friebolin, *Basic One- and Two-Dimensional NMR Spectroscopy*, WILEY-VCH, Weinheim, 4th edn, 2005.

34 (*a*) A. V. Pawlikowski, A. Ellern and A. D. Sadow, *Inorg. Chem.*, 2009, **48**, 8020–8029; (*b*) J. R. Robinson, Z. Gordon, C. H. Booth, P. J. Carroll, P. J. Walsh and E. J. Schelter, *J. Am. Chem. Soc.*, 2013, **135**, 19016–19024.

35 (*a*) T. Fueno, R. A. Shelden and J. Furukawa, *J. Polym. Sci., Part A: Polym. Chem.*, 1965, **3**, 1279–1288; (*b*) F. A. Bovey and P. A. Mirau, *NMR of Polymers*, Elsevier, 1996.

36 M. Arcana, O. Giani-Beaune, F. Schué, W. Amass and A. Amass, *Polym. Int.*, 2000, **49**, 1348–1355.

37 (*a*) N. Ajellal, D. M. Lyubov, M. A. Sinenkov, G. K. Fukin, A. V. Cherkasov, C. M. Thomas, J.-F. Carpentier and A. A. Trifonov, *Chem.–Eur. J.*, 2008, **14**, 5440–5448; (*b*) M. Bouyahyi, N. Ajellal, E. Kirillov, C. M. Thomas and J.-F. Carpentier, *Chem.–Eur. J.*, 2011, **17**, 1872–1883; (*c*) D. Pappalardo, M. Bruno, M. Lamberti and C. Pellecchia, *Macromol. Chem. Phys.*, 2013, **214**, 1965–1972; (*d*) Y. Hori and T. Hagiwara, *Int. J. Biol. Macromol.*, 1999, **25**, 237–245.

38 (*a*) X. Tang, A. H. Westlie, E. M. Watson and E. Y.-X. Chen, *Science*, 2019, **366**, 754–758; (*b*) X. Tang, A. H. Westlie, L. Caporaso, L. Cavallo, L. Falivene and E. Y. Chen, *Angew. Chem., Int. Ed.*, 2020, **59**, 7881–7890.

39 A.-C. Albertsson and I. K. Varma, *Biomacromolecules*, 2003, **4**, 1466–1486.

40 (*a*) P. Kurcok, Z. Jedlinski and M. Kowalczuk, *J. Org. Chem.*, 1993, **58**, 4219–4220; (*b*) P. Kurcok, P. Dubois and R. Jèrôme, *Polym. Int.*, 1996, **41**, 479–485; (*c*) A. Dominski, T. Konieczny, M. Zieba, M. Klim and P. Kurcok, *Polymers*, 2019, **11**, 1121.

41 (*a*) H. Morikawa and R. H. Marchessault, *Can. J. Chem.*, 1981, **59**, 2306–2313; (*b*) A. Ballistreri, D. Garozzo, M. Giuffrida, G. Impallomeni and G. Montaudo, *J. Anal. Appl. Pyrolysis*, 1989, **16**, 239–253; (*c*) M. Kunioka and Y. Doi, *Macromolecules*, 1990, **23**, 1933–1936; (*d*) H. Ariffin, H. Nishida, Y. Shirai and M. A. Hassan, *Polym. Degrad. Stab.*, 2008, **93**, 1433–1439.

42 (*a*) H. R. Kricheldorf, N. Scharnagl and Z. Jedlinski, *Polymer*, 1996, **37**, 1405–1411; (*b*) M. Kawalec, G. Adamus, P. Kurcok, M. Kowalczuk, I. Foltran, M. L. Focarete and M. Scandola, *Biomacromolecules*, 2007, **8**, 1053–1058.

43 B. M. Bachmann and D. Seebach, *Helv. Chim. Acta*, 1998, **81**, 2430–2461.

44 (*a*) H. R. Kricheldorf and N. Scharnagl, *J. Macromol. Sci., Part A: Pure Appl. Chem.*, 1989, **26**, 951–968; (*b*) P. Kurcok, M. Kowalczuk, K. Hennek and Z. Jedlinski, *Macromolecules*, 1992, **25**, 2017–2020; (*c*) Z. Jedliński, P. Kurcok and R. W. Lenz, *J. Macromol. Sci., Part A: Pure Appl. Chem.*, 1995, **32**, 797–810.

45 (*a*) T. Zeng, Q. Qian, B. Zhao, D. Yuan, Y. Yao and Q. Shen, *RSC Adv.*, 2015, **5**, 53161–53171; (*b*) K. Nie, T. Feng, F. Song, Y. Zhang, H. Sun, D. Yuan, Y. Yao and Q. Shen, *Sci. China: Chem.*, 2014, **57**, 1106–1116; (*c*) E. Grunova, E. Kirillov, T. Roisnel and J.-F. Carpentier, *Dalton Trans.*, 2010, **39**, 6739–6752; (*d*) M. A. Sinenkov, G. K. Fukin, A. V. Cherkasov, N. Ajellal, T. Roisnel, F. M. Kerton, J.-F. Carpentier and A. A. Trifonov, *New J. Chem.*, 2011, **35**, 204–212; (*e*) I. D'auria, M. Mazzeo, D. Pappalardo, M. Lamberti and C. Pellecchia, *J. Polym. Sci., Part A: Polym. Chem.*, 2011, **49**, 403–413.

46 (*a*) A. A. Neverov, T. McDonald, G. Gibson and R. S. Brown, *Can. J. Chem.*, 2001, **79**, 1704–1710; (*b*) M. Hatano and K. Ishihara, *Chem. Commun.*, 2013, **49**, 1983–1997; (*c*) R. Zeng, H. Sheng, Y. Zhang, Y. Feng, Z. Chen, J. Wang, M. Chen, M. Zhu and Q. Guo, *J. Org. Chem.*, 2014, **79**, 9246–9252.

47 (*a*) M. Shibasaki, M. Kanai, S. Matsunaga and N. Kumagai, *Acc. Chem. Res.*, 2009, **42**, 1117–1127; (*b*) J. R. Robinson, J. Gu, P. J. Carroll, E. J. Schelter and P. J. Walsh, *J. Am. Chem. Soc.*, 2015, **137**, 7135–7144; (*c*) N. Kumagai, M. Kanai and H. Sasai, *ACS Catal.*, 2016, **6**, 4699–4709.

48 J.-B. Zhu and E. Y.-X. Chen, *Angew. Chem., Int. Ed.*, 2019, **58**, 1178–1182.

49 (*a*) N. Ropson, P. Dubois, R. Jerome and P. Teyssie, *Macromolecules*, 1995, **28**, 7589–7598; (*b*) G. Montaudo, M. S. Montaudo, C. Puglisi, F. Samperi, N. Spassky, A. LeBorgne and M. Wisniewski, *Macromolecules*, 1996, **29**, 6461–6465.

50 (*a*) P. Horeglad, M. Cybularczyk, A. Litwińska, A. M. Dąbrowska, M. Dranka, G. Z. Żukowska, M. Urbańczyk and M. Michalak, *Polym. Chem.*, 2016, **7**, 2022–2036; (*b*) P. Horeglad, M. Cybularczyk, B. Trzaskowski, G. Z. Żukowska, M. Dranka and J. Zachara, *Organometallics*, 2015, **34**, 3480–3496.

51 M. Save, M. Schappacher and A. Soum, *Macromol. Chem. Phys.*, 2002, **203**, 889–899.